Optics Letters

Demonstration of 10-channel mode- and polarization-division multiplexed free-space optical transmission with successive interference cancellation DSP

Yiming Li, Zhouyi Hu,* David M. Benton, Abdallah Ali, Mohammed Patel, and Andrew D. Ellis

Aston Institute of Photonic Technology, Aston University, Birmingham, B4 7ET, UK
**Corresponding author: z.hu6@aston.ac.uk*

Received 15 February 2022; revised 28 April 2022; accepted 3 May 2022; posted 3 May 2022; published 20 May 2022

We experimentally demonstrate 10-channel mode-division multiplexed free-space optical transmission with five spatial modes, each carrying 19.6925-Gbaud dual-polarization quadrature phase shift keying signals. Strong inter-mode cross talk is observed in our commercially available photonic lantern based system when using a complete orthogonal mode set as independent channels. A successive interference cancellation based multiple-input multiple-output digital signal processing (DSP) algorithm is first applied to mitigate the inter-mode cross talk in mode-division multiplexed systems. The DSP also supports unequal transmit and receive channel numbers to further improve the cross talk resiliency. Compared to the conventional minimum mean square error DSP, the required optical signal-to-noise ratio of the successive interference cancellation DSP is decreased by approximately 5 dB at the hard-decision forward error correction limit. As a result, this system demonstrates a record-high independent channel number of 10 and spectral efficiency of 13.7 b/s/Hz in mode-division multiplexed free-space optical systems.

https://doi.org/10.1364/OL.456235

Mode-division multiplexing (MDM) is a promising technology to improve the capacity of free-space optical (FSO) communication systems [1]. By simultaneously loading independent data onto different orthogonal modes, MDM can significantly improve the transmission data rate and the spectral efficiency. In an ideal MDM system, the orthogonality among different modes guarantees negligible inter-mode cross talk. However, device imperfection, spatial misalignment, and atmospheric turbulence can lead to significant inter-mode cross talk [2–4].

To reduce the inter-mode cross talk, MDM FSO links can use a subset of the available modes with the lowest likelihood of cross talk. Orbital-angular-momentum (OAM) modes have been shown to have good cross talk resiliency during turbulent free-space transmission [5,6]. Cross talk can also be suppressed by adding a reference without OAM for adaptive optics approaches [6]. However, OAM modes are a linear combination of a strict subset of the Laguerre–Gaussian (LG) modal basis set [7]. Therefore, OAM modes suffer from significantly larger beam divergence than complete orthogonal mode sets when transmitting the same number of channels through the same sized aperture [8]. To further increase the transmission capacity, it is preferable to use a complete orthogonal mode set for MDM transmission.

Another approach to mitigate the negative effect of inter-mode cross talk is to use multiple-input multiple-output (MIMO) digital signal processing (DSP) [9]. The conventional DSP method for cross talk mitigation is minimum mean square error (MMSE) MIMO equalization [9–11]. Although MMSE MIMO equalizers can effectively recover the MIMO signals from channel matrices with mutually orthogonal column vectors, it suffers from significant performance degradation in channels with mutually non-orthogonal column vectors [12], such as those with mode dependent loss (MDL), or where not all possible modes are detected. To better compensate for the channel imperfections, advanced DSP methods, such as successive interference cancellation (SIC), are required [13].

To investigate ultimate performance limits, many experimental demonstrations of MDM FSO communication systems use a diverse range of components including, for example, beam splitters and spatial light modulators [9,14]. To reduce hardware complexity and power loss, commercially available mode sorters, such as mode-selective photonic lanterns (MSPLs) [2], can be considered as an alternative choice. Moreover, optical amplifiers can also be applied to further compensate for the power loss in the FSO channel [15]. However, such simplified systems may suffer from mode coupling effect, MDL, and mode dependent gain (MDG) from device imperfections [2,16,17].

In this Letter, we experimentally demonstrate the possibility of using a complete orthogonal mode set in an MDM FSO communication system to achieve a record-high independent

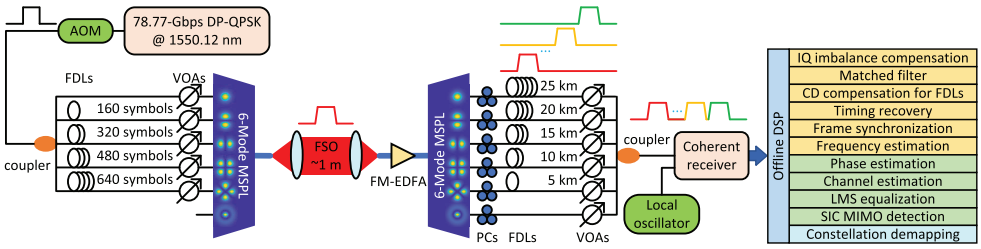

Fig. 1. Experimental setup. AOM, acousto-optic modulator; FDLs, fiber delay lines; VOAs, variable optical attenuators; MSPL, mode-selective photonic lantern; FM-EDFA, few-mode erbium-doped fiber amplifier; PCs, polarization controllers; IQ, in-phase and quadrature signals; CD, chromatic dispersion; LMS, least mean squares; SIC, successive interference cancellation.

transmit channel number of 10. The MDM system has five spatial modes with each mode carrying a 19.6925-Gbaud dual-polarization quadrature phase shift keying (DP-QPSK) signal. Different from some previous MDM FSO demonstrations [18], all of the 10 channels used in this work are independent. To achieve better system performance, SIC is first introduced in the MDM MIMO decoder for enhanced cross talk resiliency. The DSP is also designed to support unequal transmit and receive channel numbers to further mitigate the cross talk.

The experimental setup is shown in Fig. 1. The MSPLs and few-mode erbium-doped fiber amplifier (FM-EDFA) are manufactured by Phoenix Photonics Ltd. At the transmitter side, the 19.6925-Gbaud DP-QPSK signals at 1550.12 nm were generated by a Ciena WaveLogic 3 transponder, where the modulator was driven by the onboard four-channel 39.385-GSa/s arbitrary waveform generator. The signals had a pilot-aided frame structure with a frame length of 10^4 symbols, a 9.6% training sequence at the beginning of the frame, and one pilot for every nine data symbols. The training sequence and pilots were pseudo randomly generated symbols and the data symbols were based on a pseudo random binary sequence with a repeating length of 32,544. The signals were root-raised cosine shaped with a roll-off factor of 0.1. The generated signals were then passed through an acousto-optic modulator (AOM) to enable a time-division multiplexing (TDM) receiver implementation which will be detailed in the next paragraph. The signals were split into five channels and decorrelated with variable fiber delay lines (FDLs) of 0, 160, 320, 480, and 640 symbols for LP_{01}, LP_{11a}, LP_{11b}, LP_{21a}, and LP_{21b} inputs. The LP_{02} mode at the transmitter side was intentionally left unconnected because of its significantly higher loss. To compensate for the MDL of the system from the transmitter side, the delayed signals were then connected to variable optical attenuators (VOAs), which were set to ensure that each transmit channel contributed approximately equal power to the input of the FM-EDFA. Finally, the signals were spatially multiplexed into a few-mode fiber (FMF) by a six-mode MSPL and then coupled into free space using a lens with 100-mm focal length.

At the receiver side, the free-space beam was coupled into an FMF using another lens with 100-mm focal length after ~1 m FSO transmission. The signals were then amplified by an FM-EDFA and demultiplexed by another MSPL. Six polarization controllers (PCs) were connected to the output of the MSPL to balance the received power in different polarization states. Afterwards, the TDM structure was realized by the AOM at the transmitter and an array of FDLs at the receiver [11]. At the transmitter, the AOM was set to be operated at a period of 200 μs and a duty-cycle of 10%, generating a 20-μs burst of MDM data,

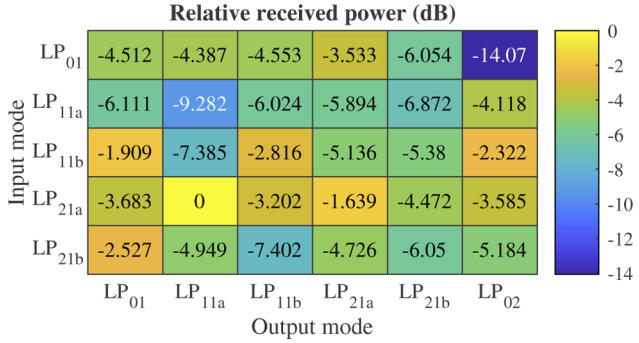

Fig. 2. Relative received power matrix of the FSO system.

which included more than 38 complete frames. At the receiver, each FDL was approximately 5 km shorter than the lower order mode (25 km for LP_{01} down to 0 km for LP_{02}), delaying the signals by approximately 24.5 μs, slightly longer than the data burst generated in the transmitter. The FDLs were then connected to six VOAs to balance the received power in different modes. By adjusting the PCs and the VOAs at the receiver, the quantization noise of the receiver can be minimized. Finally, the six mode demultiplexed and delayed signals were coupled into one single-mode fiber and received by a standard coherent receiver with 23-GHz bandwidth, 50-GSa/s sampling rate, and a standard optical signal-to-noise ratio (OSNR) scanning structure [10].

To quantify the mode cross talk in our system, Fig. 2 depicts the relative power coupling matrix of different modes. The power coupling matrix is calculated from the estimated channel matrix in the DSP. By using the pilot-aided channel estimation algorithm, we assume to produce a high-quality estimate of the channel matrix. In our system, the mode cross talk, MDL, and MDG mainly come from: (1) the imperfections and MDL in the MSPL [2]; (2) the imperfections and MDG in the FM-EDFA [16]; (3) the imperfect alignment, the mode dependent coupling loss, and the mode coupling between the linearly polarized (LP) modes in the FMF and the LG modes in the FSO channel [17].

Although the power distribution of the channel matrix can be partially compensated by the VOAs and PCs, the strong mode cross talk and MDL/MDG still leads to a channel matrix with mutually non-orthogonal column vector, which severely degrades the performance of the FSO system. To further mitigate the negative effects from the mode cross talk and the MDL/MDG, an advanced MIMO DSP, which is shown in Fig. 1, is considered in this Letter. The MIMO DSP is mainly based on the SIC algorithm to obtain enhanced cross talk resilience. However, conventional MIMO equalization algorithms can only

perform MMSE algorithm for MIMO decoding. Therefore, the conventional MIMO equalization algorithm is replaced by a sequential combination of phase estimation, channel estimation, least mean squares equalization for inter-symbol interference in time domain, and SIC MIMO detection module [19]. By doing so, the DSP can support not only different MIMO detection algorithms such as SIC and MMSE, but also different numbers of receive and transmit channels. To simplify the local oscillator setup in the coherent receiver, the DSP is also designed to support the carrier-asynchronous TDM receiver [10,19].

The schematic diagram of the SIC algorithm with N_t transmit channels and N_r receive channels is depicted in Fig. 3 [13]. When the first $i-1$ channels are successfully recovered (i.e. $\hat{s}_1, \hat{s}_2, \ldots, \hat{s}_{i-1}$), the SIC algorithm can subtract them off from the

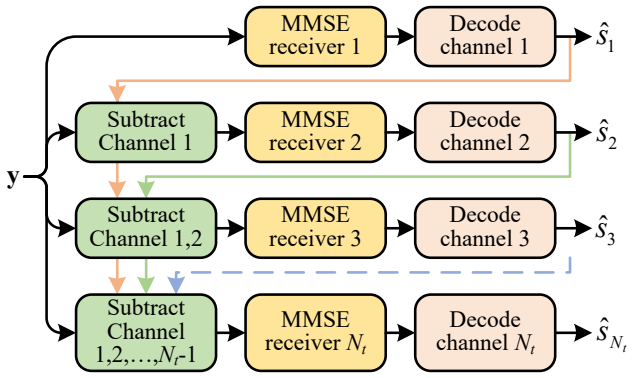

Fig. 3. Structure of the SIC algorithm. Here, $\mathbf{y}$ is the $N_r \times 1$ vector representing the N_r received channels; $\hat{s}_i$ is the estimation of the signal from the ith ($i = 1, 2, \ldots, N_t$) transmit channel.

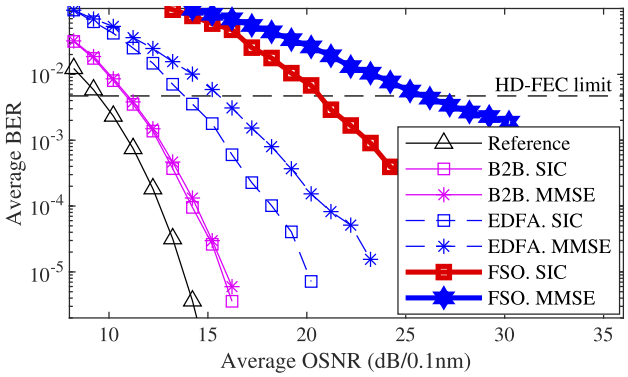

Fig. 4. Average BER curves of different 10×12 system setups. Reference, theoretical limit of ideal system; B2B, back-to-back system without FM-EDFA and FSO; EDFA, system with FM-EDFA and without FSO; FSO, full FSO system.

received signal $\mathbf{y}$. Therefore, the ith MMSE receiver can only deal with the residual channels (i.e. $s_{i+1}, s_{i+2}, \ldots, s_{N_t}$) as interference, since the first $i-1$ channels are correctly subtracted off. Moreover, the optimal decoding order for the SIC algorithm can be deduced from the estimated channel matrix [20]. Although error propagation may occur in this SIC structure, significantly better performance can be obtained by canceling out the inter-channel cross talk.

To quantify the performance degradation induced by different devices, Fig. 4 depicts the average bit error rate (BER) curves of different 10×12 system setups. In the back-to-back system without FSO and FM-EDFA, the SIC and MMSE algorithms are ~1.4 dB and ~1.5 dB worse than the ideal reference at the hard-decision forward error correction (HD-FEC) limit of 4.7×10^{-3} [21], respectively. This is mainly due to the imperfection in the MSPLs. In the system with FM-EDFA and without FSO, the SIC and MMSE algorithms are ~3.0 dB and ~4.6 dB worse than the back-to-back counterpart at the HD-FEC limit, respectively. The performance degradation mainly comes from the FM-EDFA. In the full FSO system, the SIC and MMSE algorithms are ~6.8 dB and ~10.4 dB worse than the FM-EDFA counterpart at the HD-FEC limit, respectively. This is mainly due to the imperfect coupling from the FSO channel.

To compare the performance among different MIMO algorithms (i.e. MMSE 10×10, MMSE 10×12, SIC 10×12) in the FSO system, Fig. 5 depicts the constellation with the maximum average OSNR. The SIC decoding order is LP_{21aY}, LP_{21bX}, LP_{11bY}, LP_{11bX}, LP_{21bY}, LP_{01X}, LP_{01Y}, LP_{11aY}, LP_{11aX}, LP_{21aX}. A comparison between the MMSE systems with 10 and 12 receive channels illustrates that the error vector magnitude (EVM) is smaller in all the transmit channels when more receive channels are used. This is an intuitively satisfying result as more power can be collected and more information can be extracted from the redundant receive channels. A comparison between the MMSE system and the SIC system illustrates a significant EVM performance improvement by applying the SIC algorithm. This is because that the SIC algorithm can cancel out the inter-mode cross talk. It is also worth noting that due to the nonlinear error propagation in the SIC system, the BER performance cannot be directly estimated from the EVM performance.

To compare the detailed BER performance among different MIMO algorithms in the FSO system, Fig. 6 depicts the BER curve against average OSNR. The BER of the worst channel (maximum BER) and the best channel (minimum BER) are also given in Fig. 6. Because more receive power and information are obtained from the redundant receive channels, the MMSE system with 12 receive channels outperforms the MMSE system with 10 receive channels in both the best and worst transmit channels, which results in a better average BER performance.

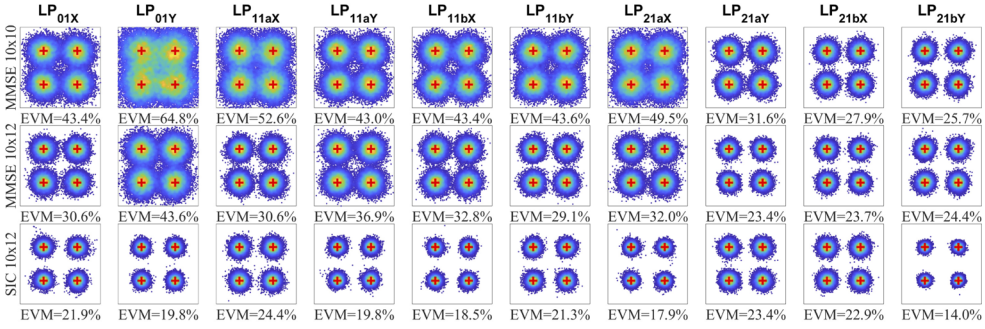

Fig. 5. Constellation for MMSE and SIC DSPs with the maximum average OSNR. Red crosses, reference QPSK constellation points.

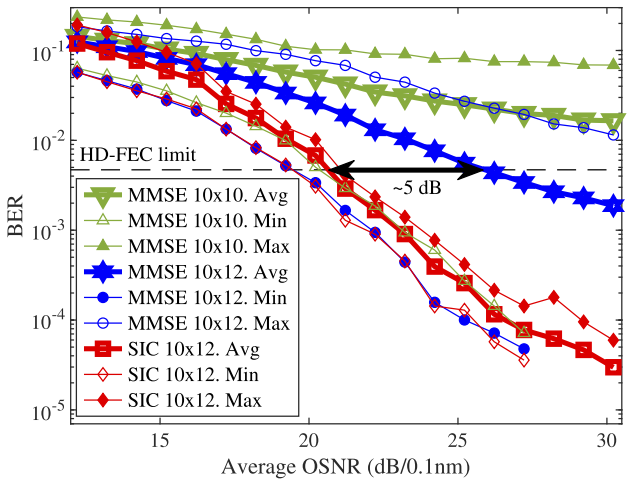

Fig. 6. BER curves of different MIMO algorithms in the FSO system. Avg, Average BER; Min, the best channel with minimum BER; Max, the worst channel with maximum BER.

Moreover, by using the redundant receive channels, the average BER of the MMSE system goes below the HD-FEC limit of 4.7×10^{-3} when the OSNR is larger than 26 dB.

When comparing the BER of the SIC and the MMSE algorithms in Fig. 6, the best channel BER of both systems are similar. This is because no cross talk cancellation is performed, and the MMSE algorithm is applied to decode the best channel in the SIC algorithm. When the best several channels have similar performance, the minimum BER may be obtained from any one of these channels, and slight BER difference may be observed. However, a significant performance improvement can be observed in the worst channel. As a result, the BER performance of all channels can go below the HD-FEC limit of 4.7×10^{-3}. This is because the worst channel is decoded in the last order when applying SIC, which cancels out all the cross talk from the other channels and therefore reduces the BER. Because the worst channel BER is the dominant factor of the average BER, the average BER of the SIC system is significantly improved and the required OSNR is approximately 5 dB less than the MMSE system at the HD-FEC limit of 4.7×10^{-3}.

In this Letter, we demonstrate a complete orthogonal mode set MDM FSO system with five modes and two polarizations using a 19.6925-Gbaud DP-QPSK signal. We only use commercially available devices in the system, which guarantees good portability to commercial applications. The strong cross talk effect in the FSO system is mitigated by our SIC DSP, and the required OSNR is approximately 5 dB smaller than the conventional MMSE DSP at the HD-FEC limit of 4.7×10^{-3}. The proposed DSP may also mitigate the turbulence-induced fading, which can be considered in the future. Considering the 10% rolloff factor, 9.6% training sequence, 10% pilot, and assuming 6.25% HD-FEC overhead, the system has a net spectral efficiency of 13.7 b/s/Hz. As a result, this system demonstrates a record-high independent channel number of 10 and spectral efficiency of 13.7 b/s/Hz in MDM FSO communication system.

Funding. H2020 Marie Skłodowska-Curie Actions (713694); Engineering and Physical Sciences Research Council (EP/S003436/1, EP/S016171/1, EP/T009047/1).

Acknowledgments. We thank Prof. Martin Lavery, Dr. Zhaozhong Chen, and Dr. Chao Gao for fruitful discussions. We also thank Ciena and Dr. Charles Laperle for kindly providing the WaveLogic 3 transponder used in our experiments.

Disclosures. The authors declare no conflicts of interest.

Data availability. Data underlying the results presented in this paper are available in Ref. [22].

REFERENCES

1. A. E. Willner, Z. Zhao, C. Liu, R. Zhang, H. Song, K. Pang, K. Manukyan, H. Song, X. Su, G. Xie, Y. Ren, Y. Yan, M. Tur, A. F. Molisch, R. W. Boyd, H. Zhou, N. Hu, A. Minoofar, and H. Huang, APL Photonics **6**, 030901 (2021).
2. A. Velazquez-Benitez, J. Alvarado, G. Lopez-Galmiche, J. Antonio-Lopez, J. Hernández-Cordero, J. Sanchez-Mondragon, P. Sillard, C. M. Okonkwo, and R. Amezcua-Correa, Opt. Lett. **40**, 1663 (2015).
3. L. Li, R. Zhang, G. Xie, Y. Ren, Z. Zhao, Z. Wang, C. Liu, H. Song, K. Pang, R. Bock, M. Tur, and A. E. Willner, Opt. Lett. **43**, 2392 (2018).
4. H. Song, R. Bock, B. Lynn, M. Tur, A. Willner, H. Song, R. Zhang, K. Manukyan, L. Li, Z. Zhao, K. Pang, C. Liu, and A. Almaiman, J. Lightwave Technol. **38**, 82 (2020).
5. G. Gibson, J. Courtial, M. J. Padgett, M. Vasnetsov, V. Pas'ko, S. M. Barnett, and S. Franke-Arnold, Opt. Express **12**, 5448 (2004).
6. Y. Ren, G. Xie, H. Huang, N. Ahmed, Y. Yan, L. Li, C. Bao, M. P. Lavery, M. Tur, M. A. Neifeld, R. W. Boyd, J. H. Shapiro, and A. E. Willner, Optica **1**, 376 (2014).
7. L. Allen, M. W. Beijersbergen, R. Spreeuw, and J. Woerdman, Phys. Rev. A **45**, 8185 (1992).
8. G. Xie, L. Li, Y. Ren, H. Huang, Y. Yan, N. Ahmed, Z. Zhao, M. P. Lavery, N. Ashrafi, S. Ashrafi, R. Bock, M. Tur, A. F. Molisch, and A. E. Willner, Optica **2**, 357 (2015).
9. H. Huang, Y. Cao, G. Xie, Y. Ren, Y. Yan, C. Bao, N. Ahmed, M. A. Neifeld, S. J. Dolinar, and A. E. Willner, Opt. Lett. **39**, 4360 (2014).
10. K. Shibahara, T. Mizuno, and Y. Miyamoto, Opt. Express **29**, 17111 (2021).
11. G. Rademacher, B. J. Puttnam, R. S. Luís, T. A. Eriksson, N. K. Fontaine, M. Mazur, H. Chen, R. Ryf, D. T. Neilson, P. Sillard, F. Achten, Y. Awaji, and H. Furukawa, Nat. Commun. **12**, 4238 (2021).
12. J. G. Proakis and M. Salehi, *Digital Communications* (McGraw-Hill, New York, 2008), 5th ed.
13. D. Tse and P. Viswanath, *Fundamentals of Wireless Communication* (Cambridge University Press, 2005).
14. Y. Ren, C. Liu, K. Pang, J. Zhao, Y. Cao, G. Xie, L. Li, P. Liao, Z. Zhao, M. Tur, R. W. Boyd, and A. E. Willner, Opt. Lett. **42**, 4881 (2017).
15. N. K. Fontaine, R. Ryf, Y. Zhang, J. C. Alvarado-Zacarias, S. van der Heide, M. Mazur, H. Huang, H. Chen, R. Amezcua-Correa, G. Li, M. Capuzzo, R. Kopf, A. Tate, H. Safar, C. Bolle, D. T. Neilson, E. Burrows, K. Kim, M. Bigot-Astruc, F. Achten, P. Sillard, A. Amezcua-Correa, and J. Carpenter, in *45th European Conference on Optical Communication (ECOC 2019)* (IET, 2019).
16. Y. Jung, E. Lim, Q. Kang, T. May-Smith, N. Wong, R. Standish, F. Poletti, J. Sahu, S. Alam, and D. Richardson, Opt. Express **22**, 29008 (2014).
17. R. Brüning, Y. Zhang, M. McLaren, M. Duparré, and A. Forbes, J. Opt. Soc. Am. A **32**, 1678 (2015).
18. H. Huang, G. Xie, Y. Yan, N. Ahmed, Y. Ren, Y. Yue, D. Rogawski, M. J. Willner, B. I. Erkmen, K. M. Birnbaum, S. J. Dolinar, M. P. J. Lavery, M. J. Padgett, M. Tur, and A. E. Willner, Opt. Lett. **39**, 197 (2014).
19. Y. Li, Z. Hu, and A. Ellis, "Crlb approaching pilot-aided phase and channel estimation algorithm in MIMO systems with phase noise and quasi-static channel fading," arXiv preprint arXiv:2112.02583 (2021).
20. J. Benesty, Y. Huang, and J. Chen, IEEE Trans. Signal Process. **51**, 1722 (2003).
21. L. M. Zhang and F. R. Kschischang, J. Lightwave Technol. **32**, 1999 (2014).
22. Y. Li, "Mode division multiplexing free space optical transmission,' (2022). https://doi.org/10.17036/researchdata.aston.ac.uk.00000536.